Dynamics of microtubule asters in microfabricated chambers: The role of catastrophes

Cendrine Faivre-Moskalenko* and Marileen Dogterom†

Institute for Atomic and Molecular Physics, Foundation for Fundamental Research on Matter, Kruislaan 407, 1098 SJ, Amsterdam, The Netherlands

Edited by J. Richard McIntosh, University of Colorado, Boulder, CO, and approved October 25, 2002 (received for review July 9, 2002)

Recent *in vivo* as well as *in vitro* experiments have indicated that microtubule pushing alone is sufficient to position a microtubule-organizing center within a cell. Here, we investigate the effect of catastrophes on the dynamics of microtubule asters within microfabricated chambers that mimic the confining geometry of living cells. The use of a glass bead as the microtubule-organizing center allows us to manipulate the aster by using optical tweezers. In the case in which microtubules preexist, we show that because of microtubule buckling, repositioning almost never occurs after relocation with the optical tweezers, although initial microtubule growth always leads the aster to the geometrical center of the chamber. When a catastrophe promoter is added, we find instead that the aster is able to efficiently explore the chamber geometry even after being relocated with the optical tweezers. As predicted by theoretical calculations, the results of our *in vitro* experiments clearly demonstrate the need for catastrophes for proper positioning in a confining geometry. These findings correlate with recent observations of nuclear positioning in fission yeast cells.

The correct positioning of microtubule (MT)-organizing centers (MTOCs) within the geometry of a living cell plays a role in a wide variety of morphological processes. These processes include positioning of the nucleus to define the future division plane of the cell and the positioning of microtubule asters during formation and orientation of the mitotic spindle (1–4). In each case, interactions of the microtubules with the confining cell membrane somehow make sure that the organizing center positions itself correctly with respect to the geometry of the cell. Although it has been shown that the molecular motor dynein is involved in many cases (5–9), there are other cases in which microtubule pushing alone seems to be sufficient to ensure proper positioning. In interphase fission yeast cells, for example, motions of the nucleus have been directly correlated with the dynamics of MTs interacting with the cell ends (10). In these experiments, the observed nuclear dynamics can be explained fully without assuming any motor activity. We have shown in previous *in vitro* experiments that simple pushing by freshly nucleated MTs indeed will allow MT asters, grown from isolated centrosomes or even MT-nucleating beads, to find the geometrical center of microfabricated chambers (11). Theoretical considerations, however, indicate that once an MT array is fully developed (or preexists), MT pushing alone does not allow the organizing center to maintain a central position or actively explore the geometry. Dynamic instability of microtubules, in the form of occasional switches (catastrophes) to a shrinking state, is expected to play an important role. Catastrophes may be needed to avoid buckling of continuously growing MTs under their own polymerization force, leading to long MTs circling around the edges of the chamber and destabilization of the central position (11). In addition, when an MT array preexists, calculations predict that efficient (fast) positioning occurs only in the presence of a sufficiently high catastrophe rate (12), regardless of the possibility of buckling.

Here, we investigate specifically the need for catastrophes in the positioning of MTOCs under conditions in which arrays of MTs preexist. We use a setup similar to our previous experiments involving artificial MTOCs (AMTOCs) and microfabricated chambers, but with the addition of optical tweezers. This allows us to manipulate the position of an organizing center after initial nucleation and growth of the MTs has taken place and study the subsequent dynamics of the system. This was not possible in our previous experiments, where positioning always occurred during the initial growth phase of freshly nucleated MTs. We show that, when using pure tubulin, repositioning almost never occurs after the MT array has developed fully, even though the geometrical center of the chamber usually is found during the initial growth phase of the MTs. When the catastrophe rate is enhanced by the addition of a catastrophe-promoting factor, we find instead that the organizing centers are able to continue to explore the geometry of the chamber even after being relocated with the optical tweezers.

Materials and Methods

Tubulin and Oncoprotein 18/Stathmin (Op18). For this study, we used tubulin purified from pig brain as described (11) as well as commercially available tubulin from Cytoskeleton (Denver). Op18 was expressed in *Escherichia coli* and purified as described (13). The protein concentration was measured by using a Bradford assay with BSA as a standard. Tubulin, as well as rhodamine-labeled tubulin, was purchased lyophilized and resuspended in MRB80 buffer (80 mM K-Pipes/1 mM EGTA/4 mM $MgCl_2$, pH 6.8) and MRB80 buffer with pH 7.5 for experiments with Op18 (14). We were unable to check directly the effect of Op18 on the dynamics of individual microtubules in our chambers. However, we verified in a regular flow cell that the addition of Op18 at the tubulin/Op18 ratio used in our experiments reduced the length of seeded MTs without reducing significantly the growth velocity, thus confirming that our Op18 was active.

Microchambers. Coverslips, cleaned with chromosulfuric acid, were spin-coated with photoresist to produce a 7.5-μm-thick layer, which then was soft-baked. The coverslips were exposed to UV through a mask and developed in the illuminated areas, leaving square islands of photoresist of 20 μm (or 30 μm) per side, separated by 10-μm-wide channels. After a hard bake, 3 μm SiO was evaporated under vacuum [4×10^{-7} torr (1 torr = 133.3 Pa)]. The remaining photoresist was dissolved in acetone. This produced square chambers of $\approx$20 μm (or 30 μm) per side and 3 μm in depth. The samples were cleaned in chromosulfuric acid and stored in air.

Optical Tweezers. A Nd:YVO4 laser beam [1,064 nm continuous wave (CW), Spectra-Physics] was introduced into a $\times$100/1.3-numerical aperture oil immersion objective (DMIRB inverted microscope; Leica, Rijswijk, The Netherlands) by using a dichroic mirror positioned below the objective. The trap position within the specimen plane was controlled by using a lens

This paper was submitted directly (Track II) to the PNAS office.

Abbreviations: MT, microtubule; MTOC, MT-organizing center; AMTOC, artificial MTOC; DIC, differential interference contrast; Op18, oncoprotein 18/stathmin.

*Present address: Centre de Recherche Paul Pascal, 115 Avenue Dr. Schweitzer, 33600 Pessac, France.

†To whom correspondence should be addressed. E-mail: dogterom@amolf.nl.

www.pnas.org/cgi/doi/10.1073/pnas.252407099

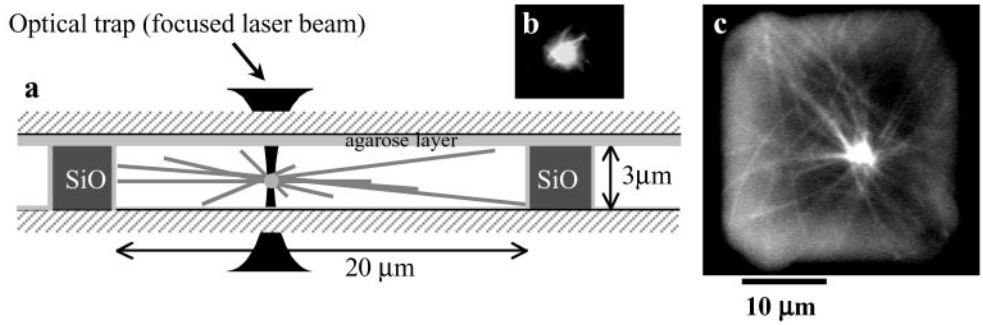

Fig. 1. (*a*) Experimental setup. The aster is grown from an AMTOC with pure tubulin and GTP and confined in a microchamber made by photolithographic techniques (SiO walls). After its first positioning, the AMTOC is trapped by using optical tweezers that allow for moving the aster away from its equilibrium position to observe repositioning. (*b*) Fluorescence image of an AMTOC in which MT nucleation seeds are attached to a 1.25-μm silica bead. (*c*) Fluorescence image of an aster positioned in the center, with buckled MTs.

mounted on an *XYZ* translation stage in a conjugate plane with the back focal plane of the objective (15). The standard laser power used to move the bead at the center of the aster was ≈300 mW in the sample. Optical damage on the MTs was never observed, and, in particular, no effect of the laser trap on the aster dynamics was detected.

AMTOCs. MTs were assembled at 37°C with a tubulin concentration of 40 μM (20% rhodamine-labeled) in a MRB80 buffer containing 2 mM GTP. To prevent extensive inter-MT crosslinking, the MTs were diluted into a 10 μM Taxol stabilizing solution. The MTs were crosslinked with 1.25 mM ethylene glycolbis (16), and, after several minutes, the reaction was quenched with 80 mM glutamic acid. To clean the MTs from the nonpolymerized tubulin, the solution was spun down through a cushion of 30% sucrose in an airfuge (Beckman Coulter) at 30 psi (1 psi = 6.9 kPa) for 30 min. The MTs were stored (up to a few weeks at room temperature) in a 50% sucrose/MRB80 solution protected from light. To obtain nucleating seeds, MTs had to be sheared with a microsyringe. To form AMTOCs, freshly sheared seeds were incubated with SiO_2 beads (COOH terminated) 1.25 μm in diameter for 10 min on a vortex machine at 400 rpm. A typical AMTOC contained between 5 and 10 MT seeds (see Fig. 1*b*). The AMTOC solution was used within 1 h.

Sample Preparation. To ensure a tight seal of the chambers, the glass slides were coated with a thin layer of agarose (dipped in 1% agarose solution at 70°C, then dried in a humidified beaker on a hot plate for 30 min and used within 1 day). The coverslips containing the microchambers also were coated with a thin layer of agarose (0.2% agarose solution at 70°C). To prevent AMTOCs from sticking to the surface, both slides were incubated for 10 min with BSA (10 mg/ml) on parafilm and air-dried. A solution containing tubulin (10% rhodamine-labeled) at a concentration varying between 11 and 36 μM, 2 mM GTP, an oxygen-scavenging system (75 mM glucose/0.6 mg/ml glucose oxidase/0.3 mg/ml catalase/7 mM dithiothreitol), and AMTOCs in MRB80 was placed on a slide. The coverslip with chambers was laid down over the solution and sealed by pressing firmly with the hand and then applying a weight (15 kg) for 4 min. The closure of the chambers was ensured by checking the fluorescence signal above the chamber walls. In practice, we managed to properly seal areas covering between 10% and 20% of the coverslip. For the experiments in the presence of Op18, the MRB80 buffer was replaced by a buffer of similar composition but with a pH adjusted to 7.5. In the final solution introduced in the sample, we estimate that the pH was between 7.3 and 7.5.

Video Microscopy Imaging and Automated Bead Tracking. Samples were observed by video-enhanced differential interference contrast (DIC) microscopy on the trapping microscope. Fluorescence microscopy was used for occasional snapshots of the MT configuration. The image was viewed by using a charge-coupled device camera (KAPPA, with digital contrast enhancement) and recorded on an S-VHS tape. The images were frame-grabbed simultaneously every second on a Silicon Graphics workstation (Mountain View, CA), and automated bead tracking (on DIC images only) was performed by using home-written software with Interactive Data Language and following previous methods (17). The position trace was obtained with subpixel resolution ($\Delta X \approx 10$ nm).

Results

To mimic the confining geometry of living cells, we made small, microfabricated chambers. By using classical photolithographic techniques, we deposited 3-μm-high SiO walls around square chambers of 20×20 or 30×30 μm^2. All chamber surfaces were coated with agarose to ensure a good seal of the chambers and also to prevent proteins from sticking. The asters were nucleated from AMTOCs consisting of 1.25-μm silica beads to which MT nucleation seeds were attached (Fig. 1*b*). The chambers were filled with a solution containing tubulin, GTP, the AMTOCs, and the necessary buffer components and then sealed with an agarose-coated slide pressed tightly to enclose the asters. The events in the chamber were monitored by video-enhanced DIC microscopy, and the bead position was detected with a home-written automated tracking program. Fluorescence microscopy was used for occasional snapshots of the MT configuration. A typical aster obtained after MT growth is shown in Fig. 1*c* and, schematically, in Fig. 1*a*.

Our first set of experiments was performed with pure tubulin, without additional catastrophe-promoting factors. We varied the tubulin concentration from 11 to 36 μM; these two extreme concentrations corresponded to situations in which none of the AMTOCs present in the sample were nucleating any MTs or to the other extreme situation, where all of the aster MTs were very long and buckled (the MTs sometimes growing in several circles along the chamber walls). For intermediate tubulin concentrations, we observed variability in the situations because of the variability in time needed to find an aster in a properly closed chamber. In contrast to our previous experiments, we chose not to include any on-stage temperature control of the sample, and MT growth, therefore, started immediately upon preparation of the sample. (Some additional variability was caused, we believe, by local inhomogeneities in surface coating, leading to variable loss of tubulin on the chamber walls.) When they were found in a closed chamber, an estimated 80% of the asters had their MTs

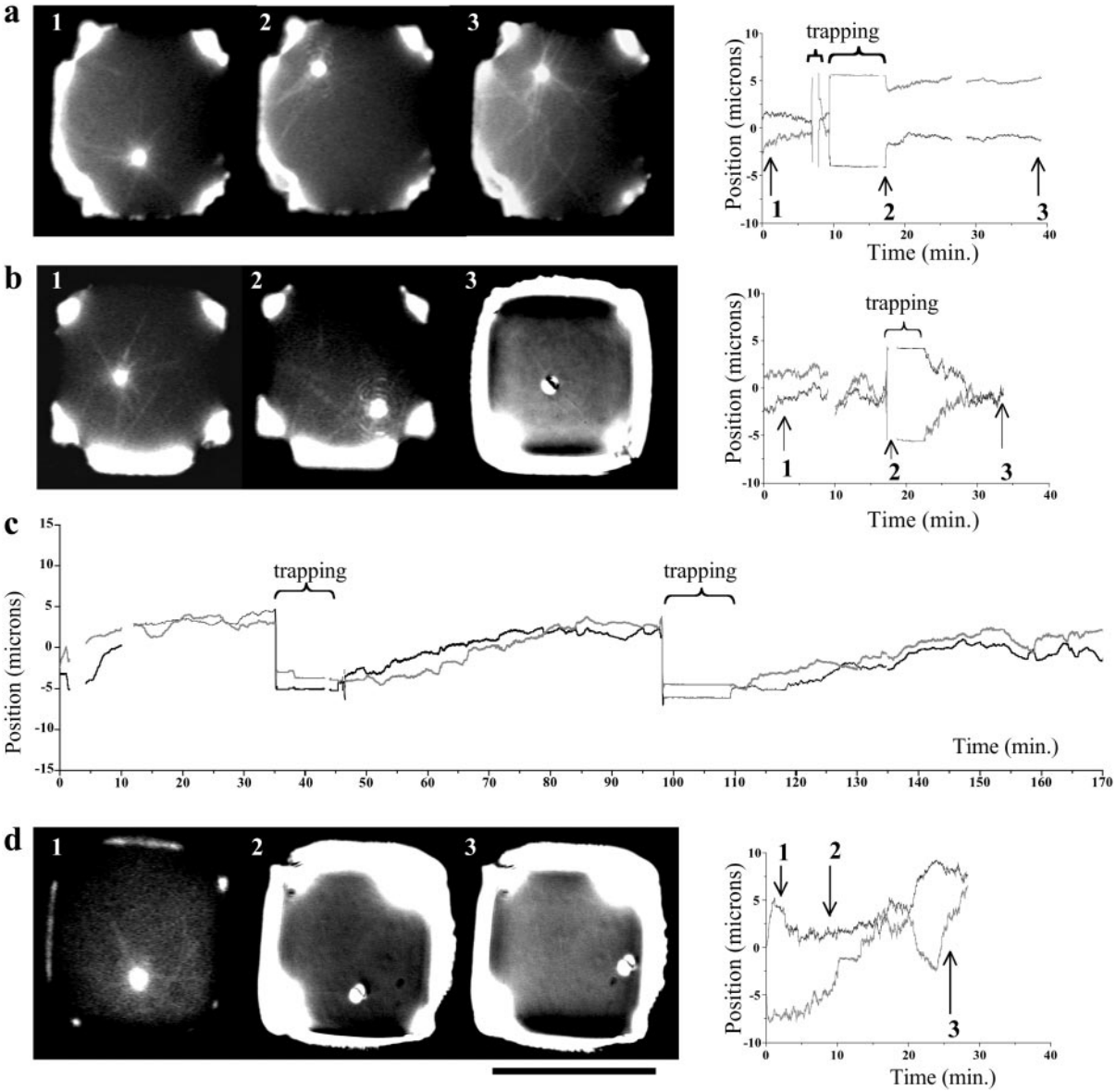

Fig. 2. (*a*) The *x* (black) and *y* (gray) coordinates plotted as a function of time for an AMTOC in a 20-μm chamber, followed with an automated position-tracking program [coordinates (0,0) indicate the middle of the chamber], when an aster first positions, then relaxes elastically after a ''short'' trapping, and, finally, does not reposition after a ''long'' trapping (because of buckling). (*b*) An aster positions and repositions after a long trapping. (*c*) An aster positions and repositions two times after a long trapping in a 30-μm chamber. (*d*) An aster exhibits large excursions in the presence of Op18. For traces *a*, *b*, and *d*, the fluorescence and DIC images show the aster for times indicated on the trace: when it is first found in the sample (1), while it is trapped (for *a* and *b*) (2), and at the end of the experiment (3). (Bar = 20 μm.)

already long and buckled (Fig. 1*c*), ≈10% of asters were actually in the process of positioning as a result of MTs growing and pushing against the chamber walls, and the last 10% were not nucleating any MTs (possibly because of a low tubulin concentration in the chamber). Keeping those numbers in mind, we now consider and analyze only the so-called ''positioning events,'' which were asters with growing MT arrays that were found early enough to still be able to move.

In Fig. 2*a*, the trace of an aster recorded for 40 min is shown. When the aster is found, a fluorescent image is taken that shows about six MTs, not yet very long. The aster positioning is observed as the MTs grow, until it has reached its equilibrium position, in this case quite close to the geometrical center of the chamber. Then, the AMTOC is trapped and the aster is moved away from the center of the chamber. If the laser trap is switched off right away, the AMTOC is seen to move back toward the center of the chamber within a few seconds, because of the elastic relaxation of the MTs, which bend when moving the aster in one corner. Hence, the aster is trapped again and held in one corner with the optical tweezers until the MTs again have reached a steady-state length distribution (or elastically adjusted to their new position). After ≈8 min, the AMTOC is released from the laser beam and the aster is seen to relax rapidly in the direction of the center over ≈2 μm and then to stay more or less in the same position (or move slowly away from the central position). A fluorescent image of the aster taken at the end of this experiment clearly shows that its MTs are long and buckled, which explains why the aster does not move anymore (see *Conclusion and Discussion*).

Similar behavior was observed for most of the asters in this first set of experiments. Of the 26 initial positioning events that

Table 1. Number of asters centering, buckling, or having large excursions, before and after trapping, in the presence or absence of Op18 (see text)

Number of asters	Total	Centered	Buckled	Large excursions
No Op18				
Before trapping	26	18	5	3
After trapping	18	4	14	0
With Op18				
Before/after trapping	13	0	0	13

we could follow, 18 asters did position relatively close to the center of the chamber (within 30% of the chamber radius), five asters got "stuck" before reaching the center because of long, buckling MTs, and the last three did not find their way to the center but exhibited large excursions within the chamber (probably as a result of a few, dynamic MTs). Of the 18 positioned asters, only four asters repositioned after trapping (two of them in a different spot than their first equilibrium position), and the majority (the other 14 asters) was prevented from moving again toward the center because of long, buckling MTs. These results are summarized in Table 1.

Fig. 2*b* shows a rare example of an aster with MTs sufficiently dynamic to allow for repositioning after trapping. The aster repositions in the same spot (close to the geometrical center of the chamber) as before trapping, and, as seen from the DIC image taken at the end of the experiment, the MTs exhibit no buckling. Unlike for the buckling aster, the fast positional fluctuations of this aster remain of similar amplitude throughout the experiment, the overall motion being notably different from free diffusion (see Fig. 3). The aster of Fig. 2*b* repositions to the center relatively quickly, in ≈7–8 min. Another example is shown in Fig. 2*c* with the trace of an aster that positions close to the center of a 30-μm chamber and is trapped to observe repositioning twice. For comparison, the time trace is plotted on the same scale as Fig. 2*b*, and it is clear that this aster repositions as well after trapping, but very slowly. The repositioning rate is of the order of 40 min. It is interesting to note that the initial positioning (where the MTs are growing for the first time) is about twice as fast (≈20 min).

In most cases, the aster repositioning was prevented by MT buckling because of, we believe, a lack of catastrophes (see *Conclusion and Discussion*). One way to increase the catastrophe rate is to decrease the tubulin concentration. However, despite our efforts, we were unable to tune the MT dynamics in a controlled way by varying only the tubulin concentration. Lowering the tubulin concentration also leads to a lower MT growth velocity and slower nucleation from the ethylene glycolbis-stabilized seeds, often leading to no aster formation at all. The intrinsic variability observed in our samples allowed us to explore the effect of changes in the MT dynamic parameters to some extent, but in a noncontrolled way (see Fig. 2 *a–c*). Another way to increase the catastrophe frequency is to use a destabilizing microtubule-associated protein. Indeed, under physiological conditions, a fast growth rate is accompanied by a high frequency of turnovers (18), a behavior never observed with pure tubulin. We chose to use Op18 (19, 20), which has been shown to promote MT catastrophes in recent *in vitro* studies (14, 21). Dependent on the pH, this protein is believed to enhance the catastrophe rate in various ways: at pH 6.8 (normal MT buffer used in our *in vitro* experiments), it seems that the main effect on the dynamic instability parameters occurs through tubulin dimer sequestering in solution, leading to a decrease of the effective tubulin concentration present in the sample. In contrast, at a higher pH of 7.5, more interesting features (for our purposes) have been observed (14): an increase of the catastrophe rate without a decrease in the growth rate.

We tested the effect of Op18 on the dynamics of MT asters and found that we had to use a combination of high tubulin and Op18 concentrations (40 and 19 μM, respectively) to obtain asters that would not show extensive MT buckling. Fig. 2*d* reports the time trace and images of an aster positioning in the presence of Op18. At the beginning of the experiment, the aster has a number of MTs similar to the previous asters in Fig. 2; that is, between 5 and 10 MTs. From the trace, it is clear that this aster exhibits larger excursions over a similar time. At first, the aster is centering, and around t = 10 min, it gets stalled for a few minutes close to the center of the chamber before it starts to move again, probably after an MT catastrophe. The aster then moves over large distances and ends up in a corner of the chamber with just a few MTs. In the presence of Op18, we followed 13 aster-positioning events (see Table 1): none experienced buckling, and all of them were moving over large distances in a directed way, sometimes centering (eight asters) but with large excursions around the geometrical center of the chamber and sometimes ending in a corner (five asters) probably because of the low number of growing MTs on the aster after the occurrence of many catastrophes. Eight asters were trapped, and, after being relocated in a corner of the chamber, they still exhibited large, continuous, directed motions, allowing them to explore large areas of the microfabricated cells but without "stable" positioning.

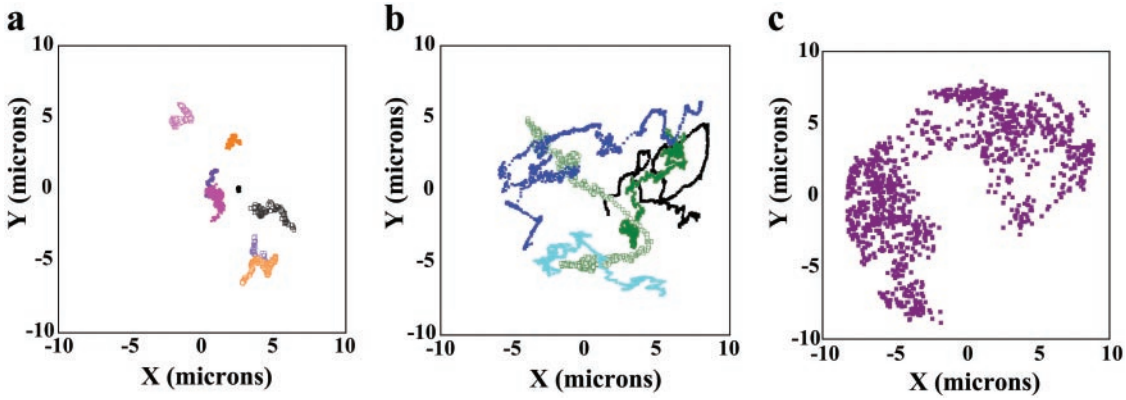

Fig. 3. The *x* and *y* plot of AMTOC motions inside 20- or 30-μm chambers. The asters were tracked for a maximum of 20 min before (filled symbols) and after (open symbols) trapping in the absence of Op18 (*a*); before (filled symbols) and after (open symbols) trapping in the presence of Op18 (*b*); and for a bead (no MTs) undergoing free diffusion (*c*).

Fig. 3 summarizes the typical differences in aster dynamics observed in the absence and presence of Op18. In the *x*–*y* plot of Fig. 3*a*, the asters are grown with pure tubulin under conditions that most often lead to buckling of the MTs. In this case, the asters are, for all practical purposes, stalled (before and after trapping). On the other hand, when a catastrophe promoter is present (Op18), the asters are highly dynamic and the MTs remain mostly straight. As shown in Fig. 3*b*, they are able to explore a large part of the chamber, with very clear, directed motions as a result of MT pushing against the surrounding walls. In both cases, the motion is very different from pure Brownian motion, which is reported in Fig. 3*c* for a freely diffusing bead.

Conclusion and Discussion

As observed (11), we find that, as it grows, an aster first moves toward a position close to the geometrical center of the chamber because of the polymerization forces generated by MTs in contact with the nearest side of the chamber. The trapping of the organizing center allows us to investigate the dynamics of positioning in the presence of preexisting MTs, where the results are qualitatively very different. When we use pure tubulin, a very low proportion of the asters actually is able to reposition near the center of the chamber after having been moved away with optical tweezers. When the catastrophe-promoting factor Op18 is added, we observe instead that the AMTOCs continuously explore a large area within the chamber.

To explain these results, we first discuss what to expect when there are no catastrophes. After initiation of growth, MTs will push the organizing center away from the first encountered barrier, with a speed equal to the growth velocity of the MTs. The actual forces generated by the MTs in this case are irrelevant (assuming the opposing drag force on the moving organizing center is small). When the organizing center approaches the center of the chamber, some of the MTs encounter the opposite barrier, and the organizing center now experiences an opposing force resulting from MTs interacting with the opposite barrier. The MTs can continue to grow only if they buckle at the same time. The elastic restoring force experienced by a buckled MT pushed against a barrier is inversely proportional to the length squared of the filament. When the MTs are long enough to buckle under their own polymerization force, they will continue to grow (at a reduced speed, depending on the magnitude of the buckling force; ref. 22) and buckle, but will not necessarily contribute to motion of the organizing center anymore. The aster gets stuck, and the position of the organizing center is determined by the balance between elastic forces (11, 23). If the force needed for buckling is too high (for short MTs), the MTs simply will stay straight and stall. In this case, the position at which contact on all sides first occurred will remain the stable position, without any further movement. Both of these situations have been observed in our previous and current experiments (in the absence of Op18). When the organizing center is relocated by using the optical trap, long MTs can form that reach all the way to the opposite barrier. Growth of these long MTs easily can overcome the critical buckling force, and the aster again gets stuck. This is what happens in most of our current experiments in the absence of Op18 (see, for example, Fig. 2*a*).

Catastrophes regulate the length of MTs and alter the length distribution compared with an array of purely growing MTs (24). For the initial positioning in a confining geometry, this does not change much, except that the number of MTs contacting the barrier at any moment may vary. The situation becomes very different as soon as there is contact with all barriers. For stiff (short) MTs that cannot buckle, the organizing center will be able to move in any direction whenever contact in that direction is lost from a catastrophe. The speed of movement again is simply the MT growth velocity until contact is reestablished and the movement is stalled. In this situation, the organizing center is constantly exploring the geometry, actively keeping its position near the center. The precision of this process depends on the number, dynamics, and length distribution of the MTs. We have shown elsewhere, by using 1D calculations and simulations, that the fastest response is possible when, on average, one MT is contacting one of the confining barriers at any time; we also have shown that typical deviations from the central position decrease with an increasing number of MTs (12).

That MTs are able to buckle does not matter much. In the "ideal" situation, the organizing center is constantly on the move around an average central position. Contact with the barrier is limited, and stalling situations producing large forces on the MTs hardly occur. In fact, this is the situation we seem to encounter when we add Op18 in our current experiments. MTs are almost never seen to buckle even though we know that they do so easily when the catastrophe rate is low. Instead, they are able to efficiently transfer the forces generated in contact with the barriers to the organizing center. The low number of MTs present on a bead in all our experiments (at most, 10 MTs) and the low nucleation events from the use of ethylene glycolbis-stabilized seeds prevent the aster from maintaining a precise position near the center (12). The motions we observe, however, clearly are caused by active exploration of the geometry and are easily distinguishable from random diffusive motion. In addition, the speeds observed during the stretches of directed motion are similar to MT growth velocities *in vitro*.

One may wonder how the "ideal" situation (namely, one MT in contact with one barrier at any time) can be reached *in vivo*. Regulation of the local (25) or global (24) catastrophe rate (by appropriate microtubule-associated proteins) may tune the average length of the MTs to the appropriate value, and the mechanism will work independently of the size of the system. In small systems, where buckling forces are large, the mechanism, in addition, may be able to self-regulate. We have shown elsewhere that catastrophes are greatly enhanced when MT growth slows down because of forces generated in interaction with a barrier.[‡] In the case of simultaneous contact with all barriers, catastrophes will be accelerated, favoring a situation in which only one MT pushes at any time. Take, for example, the positioning of the nucleus in interphase fission yeast cells. Fission yeast cells are on the order of 10 μm long and a few micrometers wide, and positioning of the nucleus occurs along the long direction of the cell by an equal number of MTs (three to four) pointing in both directions. Given the stiffness of MTs and the size of the system, one expects significant forces to develop when MTs hit both cell ends and, consequently, a significant effect on the growth dynamics of the MTs (a decrease in the growth velocity and an increase in the catastrophe rate). Both effects are observed in detailed comparison of the dynamic parameters away from and in contact with the cell ends (10, 26). The result is that MTs spend only a fraction of their time in contact with the cell ends and that catastrophes are enhanced as soon as the system stalls. A rough estimate of the number of MTs contacting the cell ends at any time can be made by using the parameters reported by Tran *et al.* (10). For a maximum cell size of 14 μm, one can calculate that each MT spends $\approx$17% of its time in contact with a cell end (the remainder of its time is spent growing and shrinking, considering that catastrophes also occur away from the cell end). Therefore, on average, 1–1.4 MTs are in contact with one of the cell ends at any time (for a total of six to eight MTs). This is pretty close to the ideal situation. It is important to stress that in this scenario it is the occurrence of sufficient catastrophes that allows the system to find the geometrical center of a confining geometry and not the balance of (length-dependent) buckling forces (10). The length distribution

[‡]Janson, M. E., de Dood, M. E., & Dogterom, M. (2001) *Mol. Biol. Cell* **12,** 173a (abstr.).

of MTs undergoing dynamic instability ensures that contact is established more often with the near cell end than with the far end, leading, on average, to more frequent motions toward than away from the cell center (if MTs are distributed symmetrically).

Our *in vitro* experiments have allowed us to show, qualitatively, the importance of catastrophes for the exploration of confining geometries. They have not allowed us, as we originally hoped, to quantitatively correlate individual MT dynamics with MTOC behavior, because it turned out to be difficult to control precisely the local tubulin concentration or follow individual MT dynamics against a highly fluorescently labeled tubulin background in the chambers. In fact, one may have a better chance to correlate these parameters *in vivo* in fission yeast cells expressing GFP-tubulin and compare WT with mutant cells that show altered MT dynamics (2). One way to improve the situation *in vitro* is to use a combination of microtubule-associated proteins that reproduces a more physiological combination of fast growth and catastrophe rates (18) and turn to chambers of smaller dimensions to suppress MT buckling. Ultimately, one then would like to add motor proteins to this system to study the interplay between two possible mechanisms of MTOC positioning, one based on MT pushing and one based on motor pulling.

We thank Marcel Janson for various forms of help in setting up the experiment; Astrid van der Horst, Wouter Roos, and Dirk Vossen for help with the optical tweezers setup; Koen Visscher for advice on this setup; Maurice van den Boer for help with the photolithography; Marco Konijnenburg for writing the Interactive Data Language tracking program; Carlos van Katz and Alfons van Blaaderen for synthesis of the beads; and Marcel Janson, Sander Tans, and Sander Piersma for critical reading of the manuscript. We thank Isabelle Arnal and Eric Karsenti for providing us with the Op18 plasmid and purification procedure and Gerbrand Koster for help with purifying Op18. This work is part of the research program of the Stichting voor Fundamenteel Onderzoek der Materie (FOM), which is supported financially by the Nederlandse Organisatie voor Wetenschappelijk Onderzoek (NWO).

1. Reinsch, S. & Gonczy, P. (1998) *J. Cell Sci.* **111,** 2283–2295.
2. Hayles, J. & Nurse, P. (2001) *Nat. Rev. Mol. Cell Biol.* **2,** 647–656.
3. Stearns, T. (1997) *J. Cell Biol.* **138,** 957–960.
4. Wittmann, T., Hyman, A. & Desai, A. (2001) *Nat. Cell Biol.* **3,** E28–E34.
5. Dujardin, D. L. & Vallee, R. B. (2002) *Curr. Opin. Cell Biol.* **14,** 44–49.
6. Adames, N. R. & Cooper, J. A. (2000) *J. Cell Biol.* **149,** 863–874.
7. Gonczy, P., Pichler, S., Kirkham, M. & Hyman, A. A. (1999) *J. Cell Biol.* **147,** 135–150.
8. O'Connell, C. B. & Wang, Y.-I. (2000) *Mol. Biol. Cell* **11,** 1765–1774.
9. Koonce, M. P., Koehler, J., Neujahr, R., Schwartz, J.-M., Tikhonenko, I. & Gerish, G. (1999) *EMBO J.* **18,** 6786–6792.
10. Tran, P. T., Marsh, L., Doye, V., Inoue, S. & Chang, F. (2001) *J. Cell Biol.* **153,** 397–411.
11. Holy, T. E., Dogterom, M., Yurke, B. & Leibler, S. (1997) *Proc. Natl. Acad. Sci. USA* **94,** 6228–6231.
12. Dogterom, M. & Yurke, B. (1998) *Phys. Rev. Lett.* **81,** 485–488.
13. Arnal, I., Karsenti, E. & Hyman, A. A. (2000) *J. Cell Biol.* **149,** 767–774.
14. Howell, B., Larsson, N., Gullberg, M. & Cassimeris, L. (1999) *Mol. Biol. Cell* **10,** 105–118.
15. Visscher, K., Gross, S. P. & Block, S. M. (1996) *IEEE J. Sel. Top. Quantum Electron.* **2,** 1066–1076.
16. Howard, J. & Hyman, A. A. (1993) in *Motility Assays for Motor Proteins*, ed. Scholey, J. M. (Academic, San Diego), pp. 105–113.
17. Gelles, J., Schnapp, B. J. & Sheetz, M. P. (1988) *Nature* **331,** 450–453.
18. Kinoshita, K., Arnal, I., Desai, A., Drechsel, D. N. & Hyman, A. A. (2001) *Science* **294,** 1340–1343.
19. Belmont, L. D. & Mitchison, T. J. (1996) *Cell* **84,** 623–631.
20. Cassimeris, L. (2002) *Curr. Opin. Cell Biol.* **14,** 18–24.
21. Curmi, P. A., Andersen, S., Lachkar, S., Gavet, O., Karsenti, E., Knossow, M. & Sobel, A. (1997) *J. Biol. Chem.* **272,** 25029–25036.
22. Dogterom, M. & Yurke, B. (1997) *Science* **278,** 856–860.
23. Holy, T. E. (1997) Ph.D. thesis (Princeton University, Princeton).
24. Verde, F., Dogterom, M., Stelzer, E., Karsenti, E. & Leibler, S. (1992) *J. Cell Biol.* **118,** 1097–1108.
25. Brunner, D. & Nurse, P. (2000) *Cell* **102,** 695–704.
26. Drummond, D. R. & Cross, R. A. (2000) *Curr. Biol.* **10,** 766–775.